A direct thin-film path towards low-cost large-area III-V photovoltaics

Rehan Kapadia[1,2,*], Zhibin Yu[1,2,*], Hsin-Hua H. Wang[1,2], Maxwell Zheng[1,2], Corsin Battaglia[1,2], Mark Hettick[1,2], Daisuke Kiriya[1,2], Kuniharu Takei[1,2], Peter Lobaccaro[2,3], Jeffrey W. Beeman[2], Joel W. Ager[2], Roya Maboudian[3], Daryl C. Chrzan[2,4], Ali Javey[1,2,†]

1. Electrical Engineering and Computer Sciences, University of California, Berkeley, CA 94720

2. Materials Sciences Division, Lawrence Berkeley National Laboratory, Berkeley, CA 94720

3. Chemical and Biomolecular Engineering, University of California, Berkeley, CA 94720

4. Materials Science and Engineering, University of California, Berkeley, CA 94720

* Authors contributed equally to the work

† Corresponding Author: ajavey@berkeley.edu

Supplementary Information
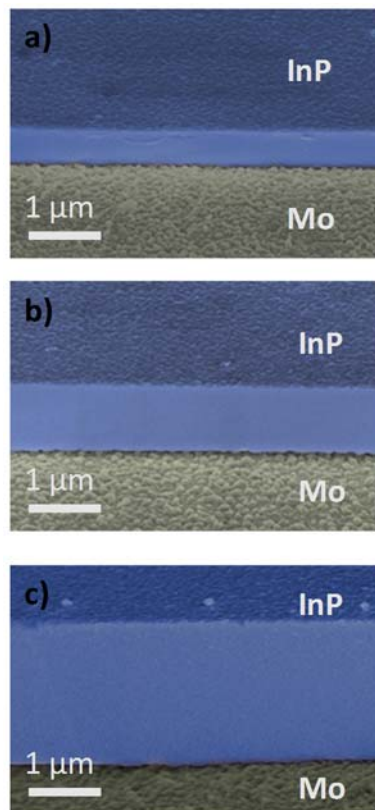
Thickness Control of TF-VLS InP

Figure S1. Thickness Control. 30° tilt view SEM images (false color) of TF-VLS grown InP of varying thickness, **a**, ~500 nm, **b**, 1 μm, **c**, 2 μm, obtained by varying the thickness of the initial indium layer (250 nm, 500 nm and 1 μm, respectively).

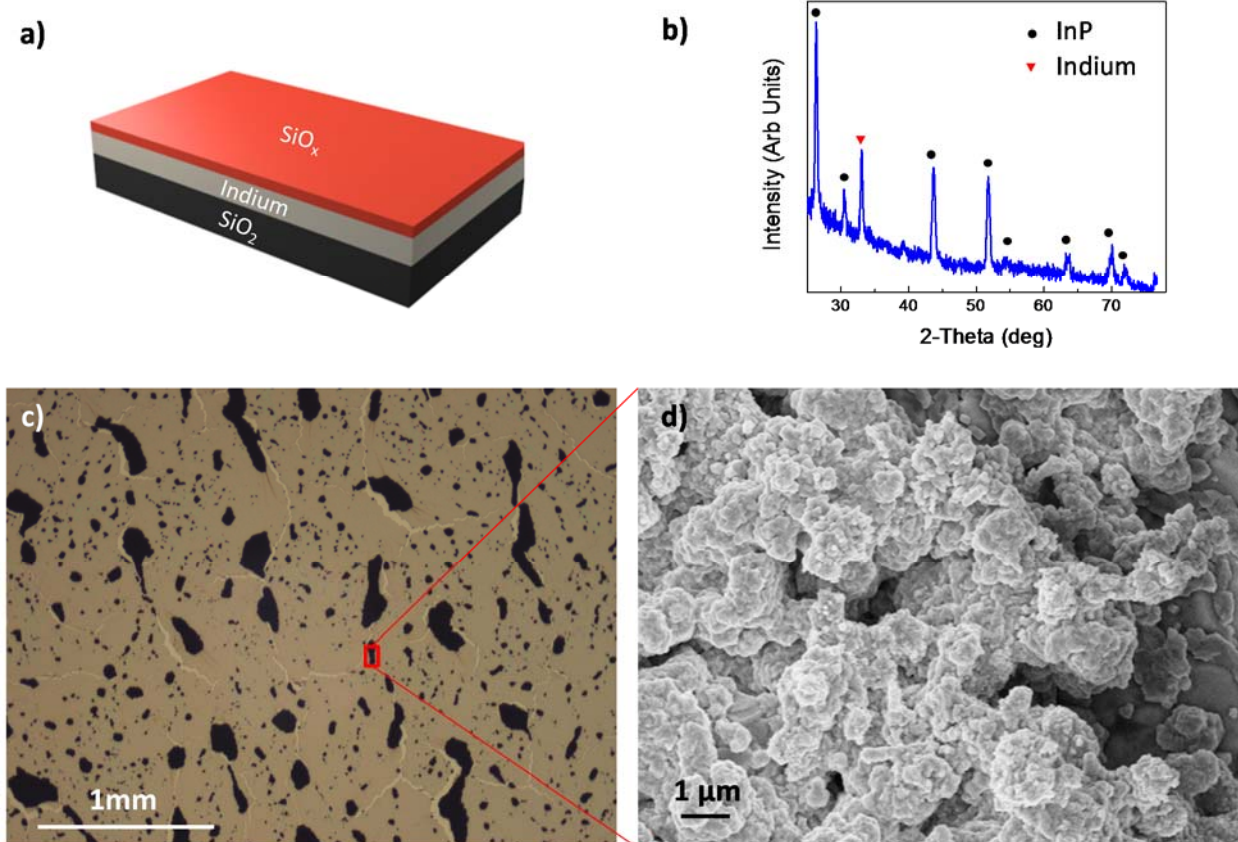**Control Experiment: Attempted phosphorization of indium on a *SiO₂ substrate***

Figure S2. Attempted phosphorization of indium on a SiO₂ substrate (instead of Mo). a, Schematic of the starting SiO₂/In/SiO₂ substrate. **b**, XRD of the substrate after attempted phosphorization at 750 °C. In contrast to samples on a Mo substrate, the large indium peak indicates that a significant portion of the indium film has not turned into InP. **c**, Optical microscope image of the substrate after exposure to phosphorous. The indium clearly dewets from the SiO₂ surface, indicating that the surface energies of both sides of the template are high. **d**, SEM image of the resulting film showing morphology of the In/InP clumps. These results show that InP does not nucleate effectively on SiO₂.

Control Experiment: Phosphorization of indium *without* a SiO$_x$ cap layer
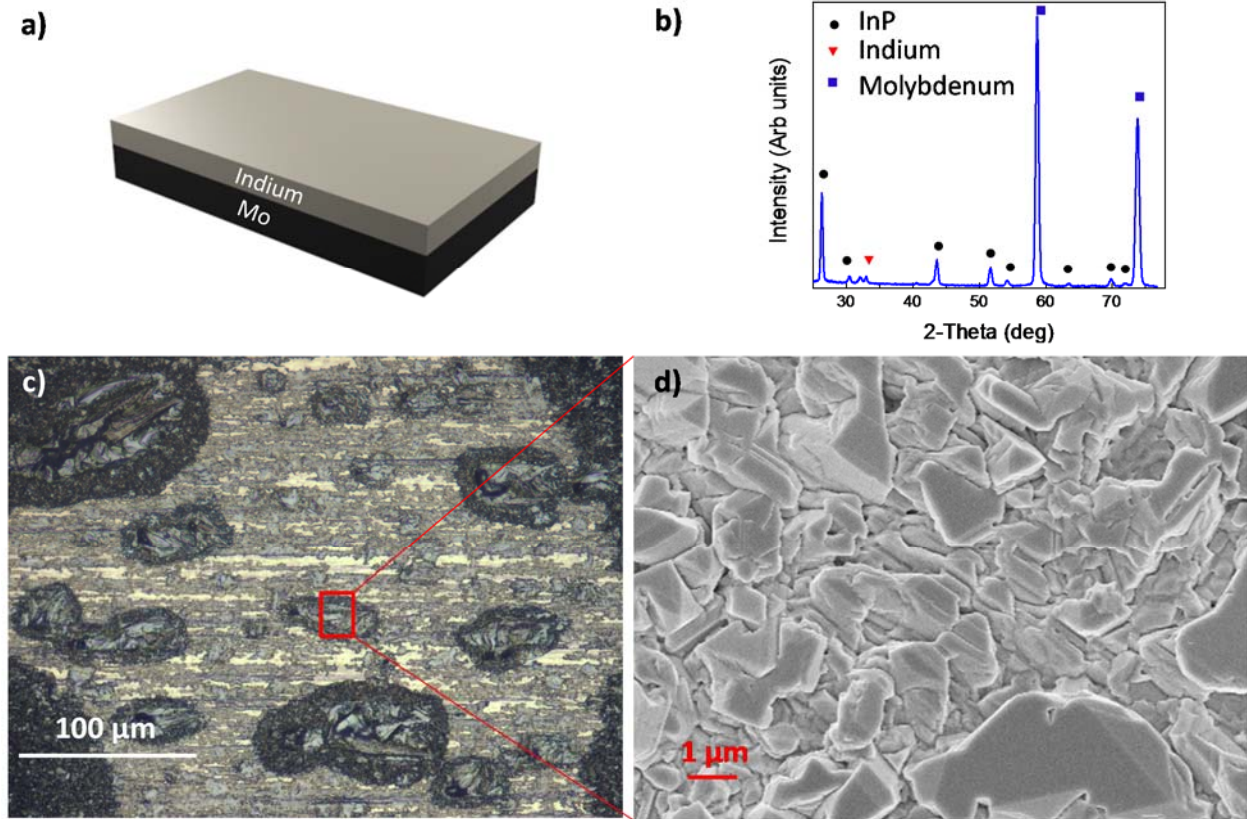

Figure S3. Phosphorization of indium without a cap. a, Schematic of a starting In/Mo substrate. **b**, XRD of In phosphorized *without* a SiO$_x$ cap, depicting that majority of the indium has turned into InP. Trace amount of indium was left due to indium dewetting to form large aggregates which became difficult to fully phosphorize under the explored growth conditions. **c**, Optical microscope image of indium phosphorized without a cap. In contrast to TF-VLS growth *with* a SiO$_x$ cap, indium clearly dewets from the Mo surface. **d**, SEM image of InP showing significantly smaller grain sizes compared to the TF-VLS grown InP *with* a cap. This is attributed to the much larger flux of P into the liquid indium during phosphorization *without* a cap.
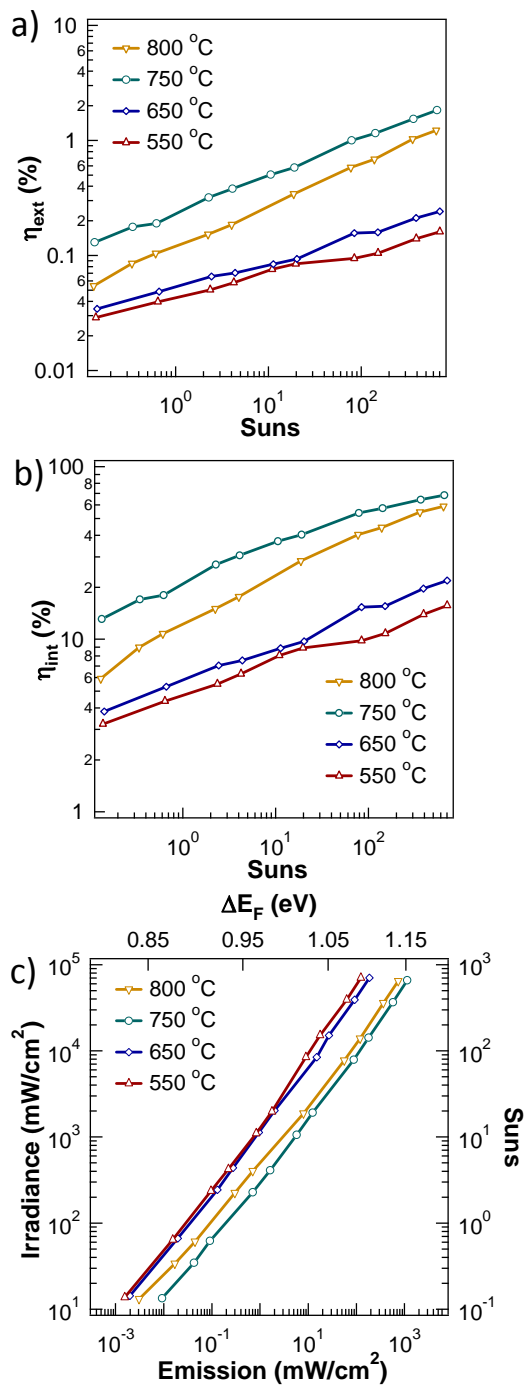
Luminescence Yield

Figure S4: Luminescence Yield. a, The measured external luminescence efficiency as a function of incident photon intensity for multiple growth temperatures. **b**, The extracted internal luminescence efficiency as a function of incident photon intensity for different growth temperatures. **c,** Photons-in vs. photons-out curves for each growth temperature. The emission intensity is correlated to the quasi Fermi level splitting as discussed in the Methods section.
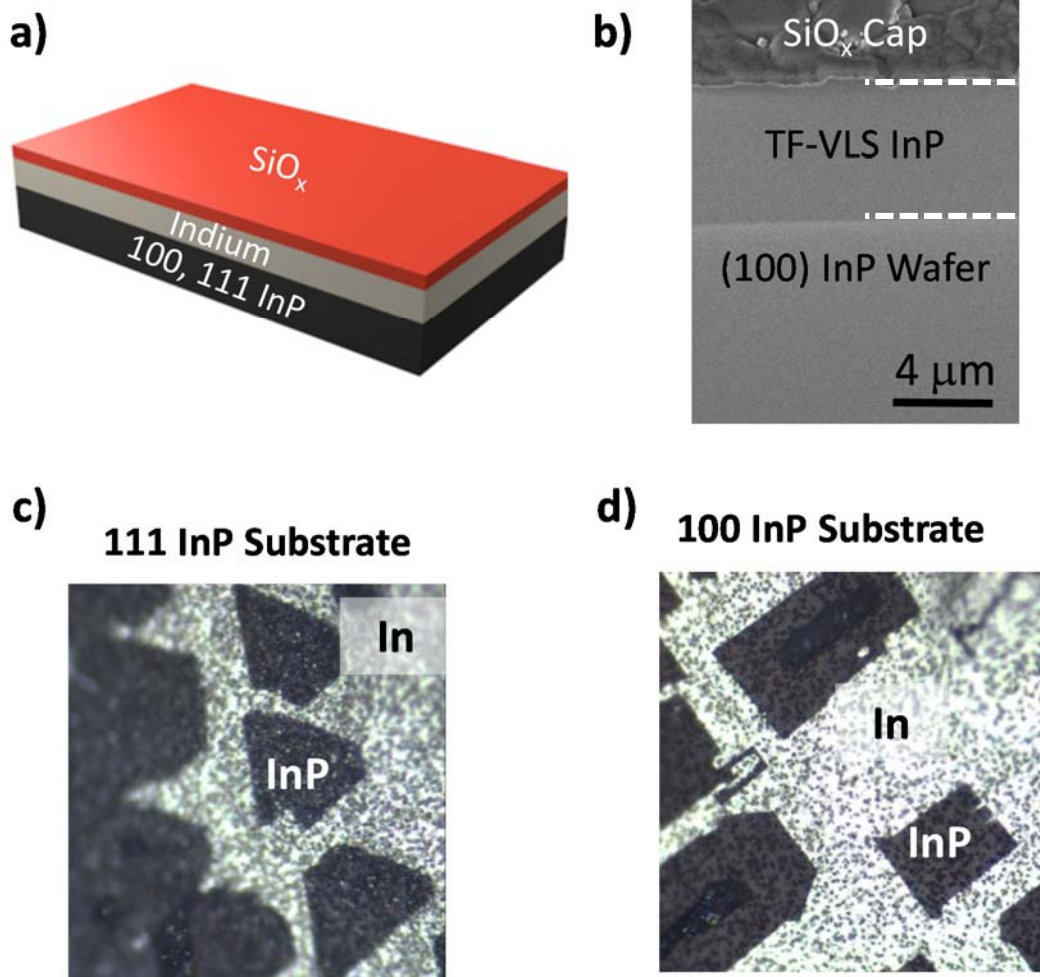
Single-Crystal InP TF-VLS Growth

Figure S5: InP Epilayer Growth by VLS. a, Schematic of the initial growth stack. **b**, Cross-sectional SEM image of a fully grown (i.e., continuous) InP thin film grown on a (100) InP wafer using the TF-VLS process. **c, d,** Optical microscope images of *partially* grown InP on (111) and (100) InP substrates, respectively. The optical images depict the epitaxial relationship of the InP islands with the underlying substrate. Here the growth is stopped short on purpose to clearly depict the nucleation islands for each crystal orientation substrate.

Growth Scaling Law

The modeling of nucleation and growth poses a substantial theoretical challenge. However, certain scaling laws can be derived through simple arguments. In the present case, we wish to understand how experimentally controllable parameters might influence the density of nuclei we form during TF-VLS growth. We can construct and analyze simple coupled differential equations that govern the process, and use their solutions to guide our growth conditions.

We begin by assuming that phosphorous enters the liquid indium film at a steady state flux of F atoms/(cm^2-sec). We assume that the initial film thickness is h (in cm). One can define a characteristic time τ by the product $\tau = \left(F h^2 \right)^{-1}$. Scaling all lengths in the problem by h, and scaling all times in the problem by τ, one can develop a dimensionless theory for the number of nuclei per unit volume. Let the dimensionless number density of nuclei in the film be N, and the dimensionless number density of excess P atoms (i.e. the number density P of atoms beyond the solubility limit) still within the liquid be n. Further, suppose that the critical nucleus contains η atoms and consequently, the nucleation rate depends on the excess concentration of P atoms raised to the power $\eta \geq 2$. The dimensionless equations governing growth can be written as:

$$\frac{dN}{d\theta} = \tilde{D}\sigma_1 n^{\eta}$$

$$\frac{dn}{d\theta} = 1 - \tilde{D}\bar{\sigma} n N - \eta \tilde{D}\sigma_1 n^{\eta}$$

(S1)

where $\tilde{D}$ is the dimensionless diffusivity of P in the liquid In, σ_1 is a dimensionless parameter describing the capture cross section of the excess P atoms in the liquid by other P atoms in the liquid to form a new nucleus, $\bar{\sigma}$ is a dimensionless capture length characterizing the capture of the excess P atoms by the existing nuclei, and θ is the dimensionless time.

In the limit that nucleation has saturated one can assume a nearly steady state condition in which $\frac{dn}{d\theta} \approx 0$, and $\tilde{D}\bar{\sigma}nN \ll \eta\tilde{D}\sigma_1 n^{\eta}$. Under these conditions, Eqs. (S1) can be integrated to yield:

$$N = \left[(1+\eta)\tilde{D}^{1-\eta} \frac{\sigma_1}{\bar{\sigma}^{\eta}} \theta + C \right]^{\frac{1}{1+\eta}} \tag{S2}$$

with C as the constant of integration. Assuming that the first term dominates the expression (certainly true in the case $\eta = 2$), the number of nuclei scales with $\tilde{D}^{\frac{1-\eta}{1+\eta}}$. Expressing the dimensionless diffusivity in terms of dimensioned quantities, one finds $\tilde{D} = \frac{D}{Fh^4}$ with D being the dimensioned diffusivity of P in the indium liquid. Rearranging, one concludes that the number density of nuclei scales according to:

$$N = \frac{A}{h^2} \left(\frac{Fh^4}{D} \right)^{\alpha} \tag{S3}$$

with $\alpha = \frac{\eta-1}{\eta+1}$, and defining $\frac{A}{h^2}$ as the proportionality constant. It should be noted that A is related to the capture cross section of P atoms by other atoms to form new nuclei (σ_1) as well as the capture length of P by existing InP islands ($\bar{\sigma}$).

In order to calibrate the model with experimental data, a set of controlled experiments were performed with two different starting indium film thicknesses of 0.5 and 3 µm. The findings are presented in Figure 3c. Specifically, by performing partial growths at different PH$_3$ partial pressures, the effect of P flux on the nucleation density of InP was probed. To fit the experimental data with the model, it is necessary to first extract the incident flux for each sample. The method for extracting flux presented here assumes (i) a constant P flux through the experiments and (ii) once In turns to InP the diffusion of P through InP is negligible compared to P diffusion through In. This enables us to write an equation for the change in fractional coverage as a function of growth time and flux:

$$\frac{d\theta}{dt} = F \left(\frac{M_{In}}{h \, N_A \, \rho_{In}} \right) (1 - \theta) \tag{S4}$$

Solving this equation and rearranging for F enables us to estimate the flux as $F = \frac{-h \, \rho_{In} \, N_A Log(1-\theta)}{M_{In} \, t}$, where ρ_{In} is the density of indium, N_A is the Avogadro constant, θ is the areal fractional coverage of the InP, M_{In} is the molar mass of indium, t is the time elapsed and h is the starting indium height.

To calibrate the nucleation density model described above (equation S3), with the experimental data, two variables were used as fitting parameters: A and α. Fitting this model to the experimental data we find that $\alpha = 0.6$ (corresponding to $\eta = 4$) and $A = 9.25 \times 10^{-9}$ for both datasets (h = 500 nm and h = 3 µm).